Supplement of Atmos. Chem. Phys., 18, 5455–5466, 2018
https://doi.org/10.5194/acp-18-5455-2018-supplement

Atmospheric Chemistry and Physics
Open Access

Supplement of

Studying volatility from composition, dilution, and heating measurements of secondary organic aerosols formed during α-pinene ozonolysis

Kei Sato et al.

Correspondence to: Kei Sato (kei@nies.go.jp)

Table S1. Molecules detected as sodium adduct ions during offline positive electrospray ionization analysis of α-pinene ozonolysis SOA samples.

Monomers			Dimers		
Formula	*m/z*	Carbon oxidation state	Formula	*m/z*	Carbon oxidation state
$C_8H_{12}O_4$	195.0628	-0.50	$C_{16}H_{24}O_6$	335.1465	-0.75
$C_8H_{12}O_5$	211.0577	-0.25	$C_{16}H_{24}O_7$	351.1414	-0.63
$C_8H_{12}O_6$	227.0526	0.00	$C_{16}H_{24}O_8$	367.1363	-0.50
$C_8H_{12}O_7$	243.0475	0.25	$C_{17}H_{26}O_6$	349.1622	-0.82
$C_8H_{14}O_5$	213.0733	-0.50	$C_{17}H_{26}O_7$	365.1571	-0.71
$C_8H_{14}O_6$	229.0683	-0.25	$C_{17}H_{26}O_8$	381.152	-0.59
$C_8H_{14}O_7$	245.0632	0.00	$C_{17}H_{26}O_9$	397.1469	-0.47
$C_9H_{14}O_3$	193.0835	-0.89	$C_{17}H_{26}O_{10}$	413.1418	-0.35
$C_9H_{14}O_4$	209.0784	-0.67	$C_{17}H_{26}O_{11}$	429.1367	-0.24
$C_9H_{14}O_5$	225.0733	-0.44	$C_{17}H_{28}O_6$	351.1778	-0.94
$C_9H_{14}O_6$	241.0683	-0.22	$C_{17}H_{28}O_7$	367.1727	-0.82
$C_9H_{14}O_7$	257.0632	0.00	$C_{17}H_{28}O_8$	383.1676	-0.71
$C_9H_{14}O_8$	273.0581	0.22	$C_{17}H_{28}O_9$	399.1626	-0.59
$C_9H_{16}O_5$	227.089	-0.67	$C_{17}H_{28}O_{10}$	415.1575	-0.47
$C_9H_{16}O_6$	243.0839	-0.44	$C_{17}H_{30}O_5$	337.1985	-1.18
$C_9H_{16}O_7$	259.0788	-0.22	$C_{17}H_{30}O_6$	353.1935	-1.06
$C_9H_{16}O_8$	275.0737	0.00	$C_{17}H_{30}O_7$	369.1884	-0.94
$C_{10}H_{14}O_5$	237.0733	-0.40	$C_{17}H_{30}O_8$	385.1833	-0.82
$C_{10}H_{14}O_6$	253.0683	-0.20	$C_{17}H_{32}O_5$	339.2142	-1.29
$C_{10}H_{14}O_7$	269.0632	0.00	$C_{17}H_{32}O_6$	355.2091	-1.18
$C_{10}H_{16}O_3$	207.0992	-1.00	$C_{17}H_{32}O_7$	371.204	-1.06
$C_{10}H_{16}O_4$	223.0941	-0.80	$C_{17}H_{32}O_8$	387.1989	-0.94
$C_{10}H_{16}O_5$	239.089	-0.60	$C_{17}H_{32}O_9$	403.1939	-0.82
$C_{10}H_{16}O_6$	255.0839	-0.40	$C_{18}H_{28}O_5$	347.1829	-1.00
$C_{10}H_{16}O_7$	271.0788	-0.20	$C_{18}H_{28}O_6$	363.1778	-0.89
$C_{10}H_{16}O_8$	287.0737	0.00	$C_{18}H_{28}O_7$	379.1727	-0.78
$C_{10}H_{16}O_9$	303.0687	0.20	$C_{18}H_{28}O_8$	395.1676	-0.67
$C_{10}H_{18}O_5$	241.1046	-0.80	$C_{18}H_{28}O_9$	411.1626	-0.56
$C_{10}H_{18}O_6$	257.0996	-0.60	$C_{18}H_{28}O_{10}$	427.1575	-0.44
$C_{10}H_{18}O_7$	273.0945	-0.40	$C_{18}H_{28}O_{11}$	443.1524	-0.33
$C_{10}H_{18}O_8$	289.0894	-0.20	$C_{18}H_{30}O_8$	397.1833	-0.78
$C_{10}H_{18}O_9$	305.0843	0.00	$C_{18}H_{30}O_9$	413.1782	-0.67
			$C_{18}H_{32}O_4$	335.2193	-1.33
			$C_{18}H_{32}O_5$	351.2142	-1.22
			$C_{18}H_{32}O_6$	367.2091	-1.11
			$C_{18}H_{34}O_5$	353.2298	-1.33
			$C_{18}H_{34}O_6$	369.2248	-1.22
			$C_{18}H_{34}O_8$	401.2146	-1.00
			$C_{19}H_{28}O_6$	359.1829	-0.84
			$C_{19}H_{28}O_7$	391.1727	-0.74
			$C_{19}H_{28}O_8$	407.1676	-0.63
			$C_{19}H_{28}O_9$	423.1626	-0.53
			$C_{19}H_{28}O_{10}$	439.1575	-0.42
			$C_{19}H_{28}O_{12}$	471.1473	-0.21
			$C_{19}H_{30}O_5$	361.1985	-1.05
			$C_{19}H_{30}O_6$	377.1935	-0.95
			$C_{19}H_{30}O_7$	393.1884	-0.84
			$C_{19}H_{30}O_8$	409.1833	-0.74
			$C_{19}H_{30}O_9$	425.1782	-0.63
			$C_{20}H_{30}O_6$	389.1935	-0.90
			$C_{20}H_{30}O_8$	421.1833	-0.70
			$C_{20}H_{30}O_9$	437.1782	-0.60
			$C_{20}H_{30}O_{10}$	453.1731	-0.50
			$C_{20}H_{32}O_5$	375.2142	-1.10
			$C_{20}H_{32}O_7$	407.204	-0.90
			$C_{20}H_{32}O_8$	423.1989	-0.80
			$C_{20}H_{32}O_9$	439.1939	-0.70

Table S2. Saturation concentrations determined for α-pinene oxidation products by SPARC calculations and three parameterization methods.

Compound	$\log_{10}$ (Saturated concentration / μg m^{-3})			
	SPARC (Sato et al., 2016)	1D-fit for α-pinene oxidation products (Shiraiwa et al., 2014)	2D-fit for oxygenated organic compounds (Li et al., 2016)	Binary fit for α-pinene oxidation products
pinonic acid	2.25	3.3	4.3	2.57
pinic acid	-0.75	3.2	3.81	2.37
10-hydroxypinonic acid	-0.82	2.44	3.5	1.02
MBTCA	-0.43	2.24	1.97	0.63
$C_{10}H_{16}O_5$	-	1.59	2.59	-0.53
$C_{10}H_{16}O_6$	-	0.74	1.58	-2.08
$C_{10}H_{16}O_7$	-	-0.11	0.5	-3.63
dimer of MW 348 (isomer 1)	-6.31	-5.45	-0.84	-4.62
dimer of MW 348 (isomer 2)	-7.4	-5.45	-0.84	-4.62

Table S3: Average $\log_{10} C^*$ values determined from present volatility distributions; all values are lower than the average $\log_{10} C^*$ determined from yield curves, 2.26.

	LC/MS-1D	LC/MS-2D	LC/MS-binary	LC/MS-1D w/o transmission corr.	TD-AMS	Dilution
Run 1	-2.71	-0.61	-2.76	-3.35	1.03	-
Run 2	-	-	-	-	0.16	-
Run 3	-	-	-	-	0.24	-
Run 4	-	-	-	-	0.14	-
Run 5	-	-	-	-	0.75	-
Run 6	-1.94	-0.25	-2.42	-2.66	1.32	-
Run 7	-1.89	0.10	-2.45	-2.56	1.07	-
Run 8	-1.41	0.87	-2.30	-2.02	0.99	-
Run 9	-0.83	1.44	-2.19	-1.38	0.40	-
Run 11	-	-	-	-	1.27	-
Dilution (RH <1%)	-	-	-	-	-	1.00
Dilution (RH ~40%)	-	-	-	-	-	1.60

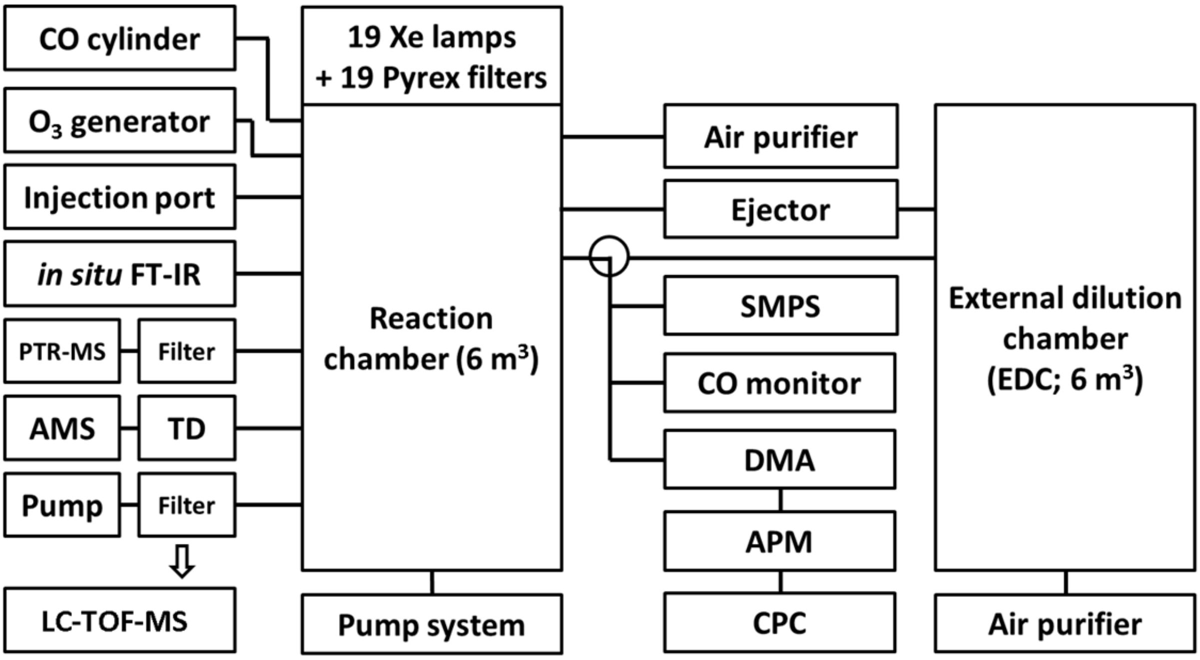

Figure S1: Schematic diagram of the chamber system and analytical instruments used for the experiments at RH <1%; a Teflon bag was used instead of the reaction chamber with the pump system for the experiments at RH ~40%. The RH of the EDC was set to ~40% when particles formed at ~40%, whereas it was set to <1% when particles formed at <1%.

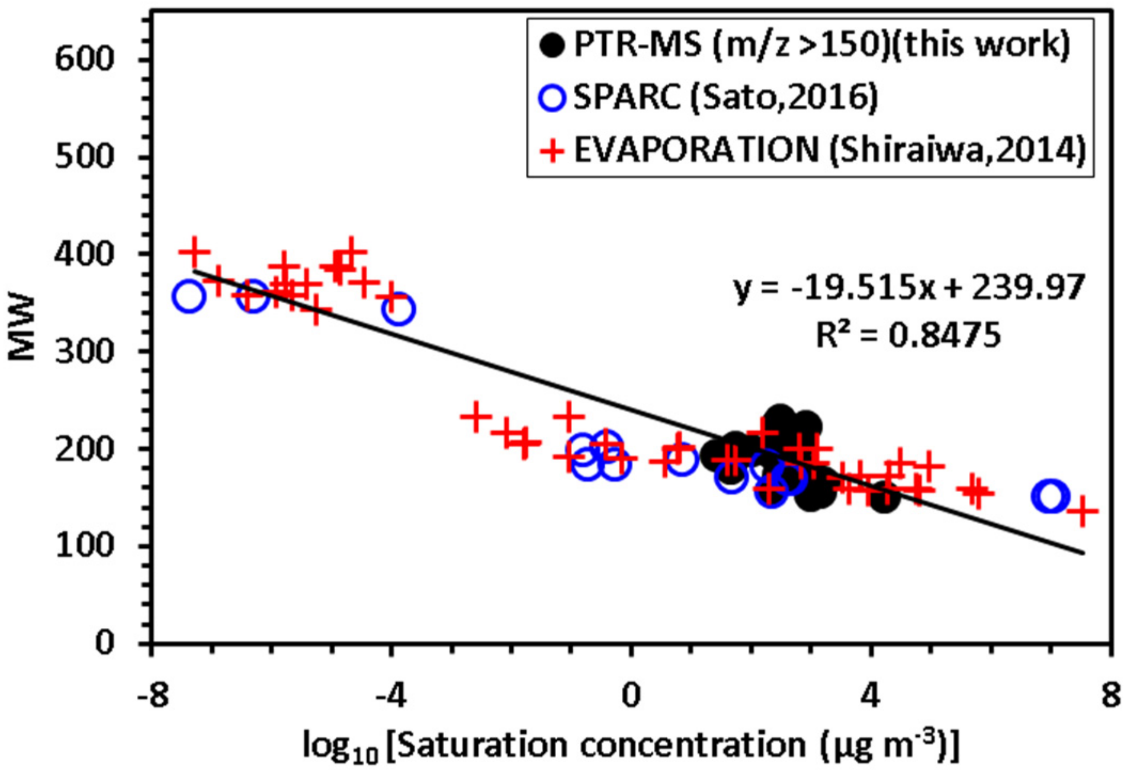

Figure S2: Molecular weight (MW) plotted as a function of $\log_{10}$ C^*: Results of PTR-MS measurements, SPARC calculations, and EVAPORATION calculations; the black line indicates the regression function fitted to the EVAPORATION data.

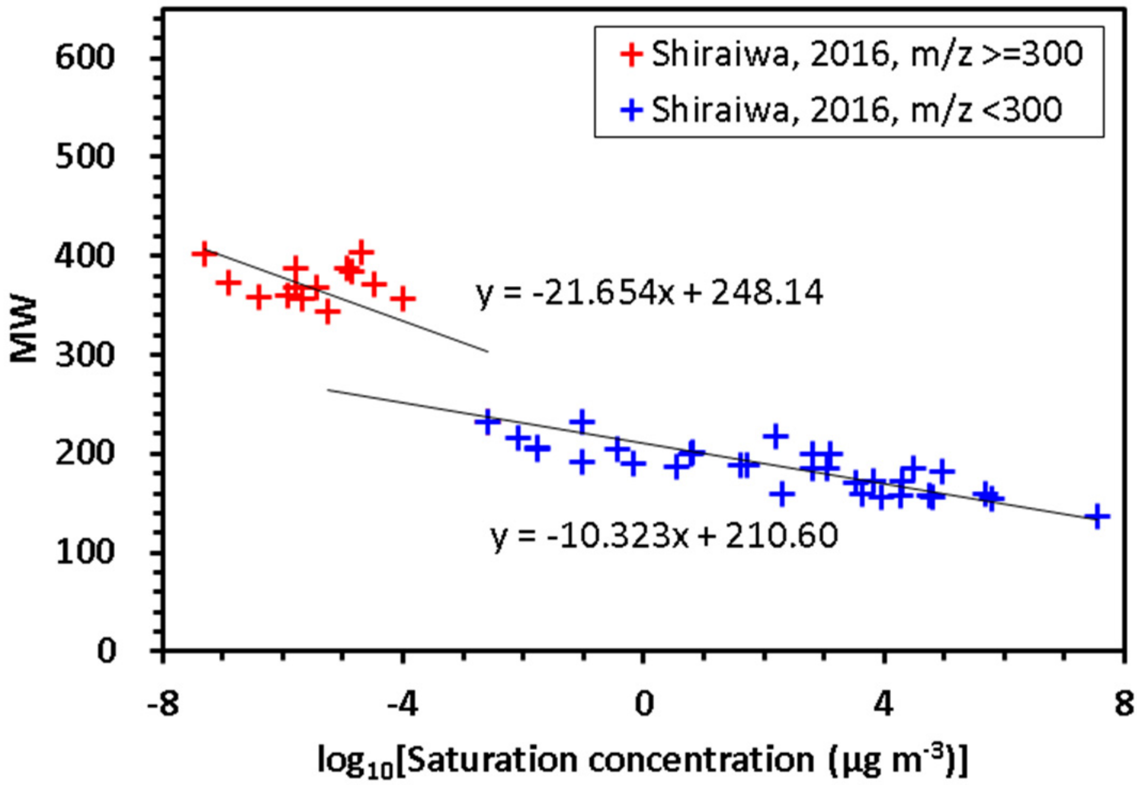

Figure S3: Molecular weight (MW) plotted as a function of $\log_{10} C^*$; straight lines are the results of binary parameterization and are fitted to data of m/z ≥300 and <300 separately.

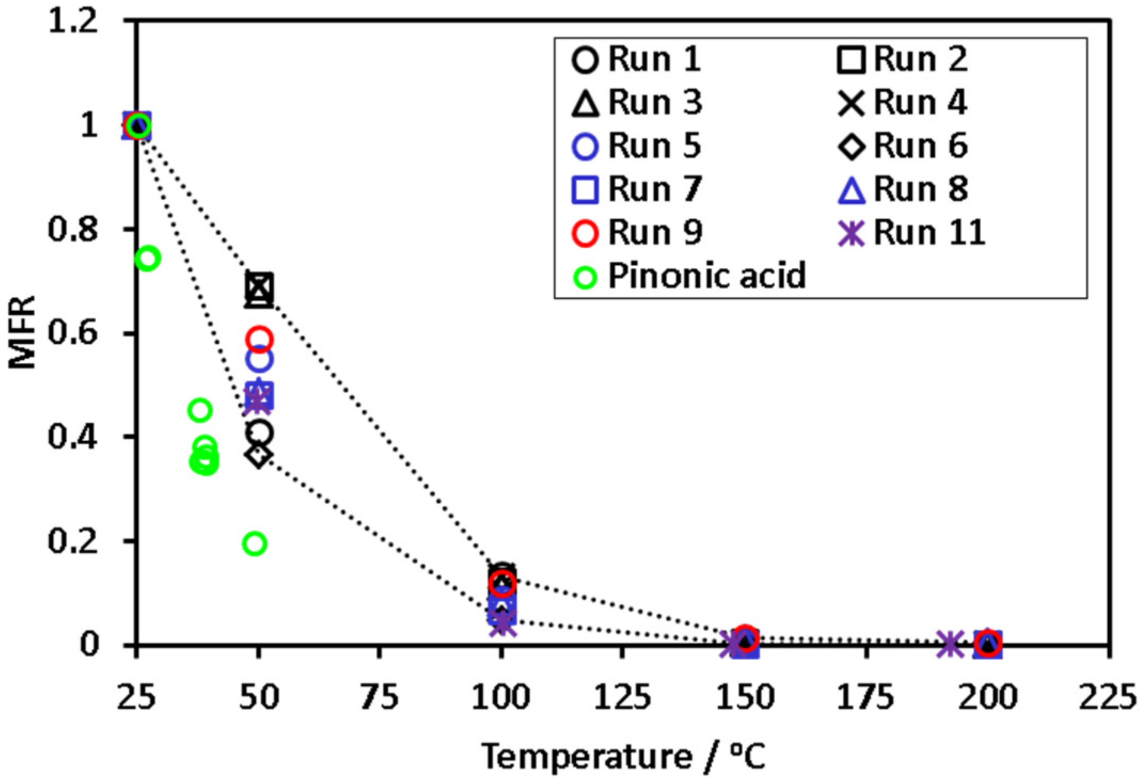

Figure S4: Mass fraction remaining (MFR) measured for SOA and pinonic acid particles as a function of thermodenuder temperature.

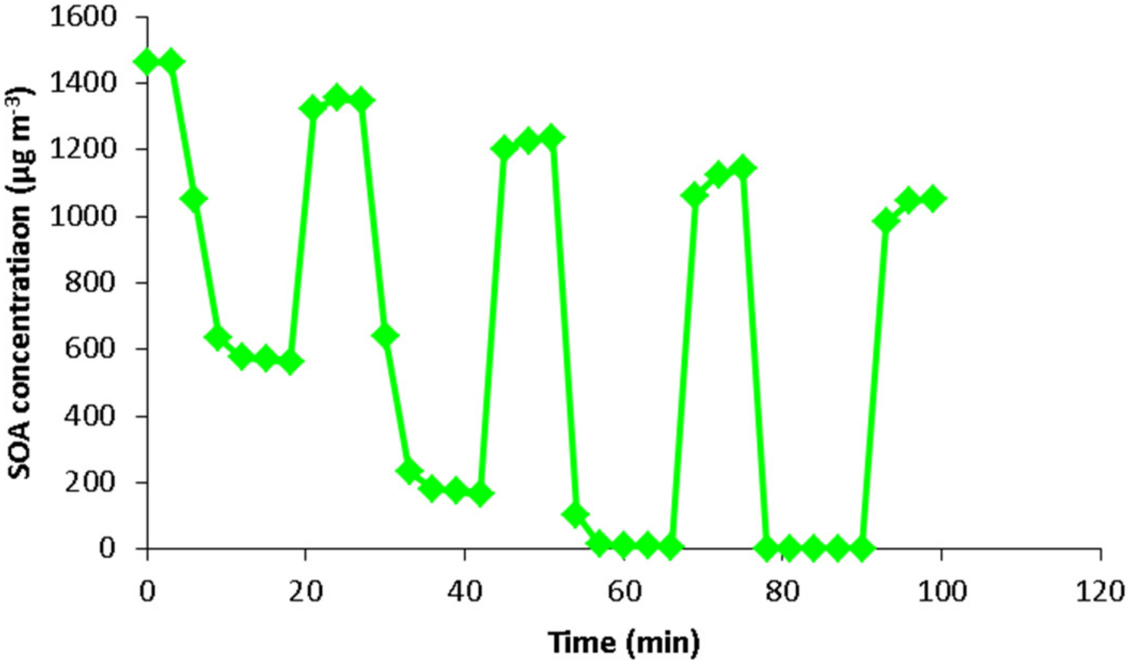

Figure S5: Time series of SOA concentration measured by TD-AMS during the heating measurement in run 1; the TD mode was programmed to be bypass (0-3 min), TD of 50°C (3-18 min), bypass (18-27 min), TD of 100°C (27-42 min), bypass (42-51 min), TD of 150°C (51-66 min), bypass (66-75 min), TD of 200°C (75-90 min), and bypass (90-99 min). The SOA concentration measured through the bypass decreased by 5-9% due to the SOA loss on the chamber wall during each measurement cycle (24 min). MFR was determined by accounting for SOA wall loss.

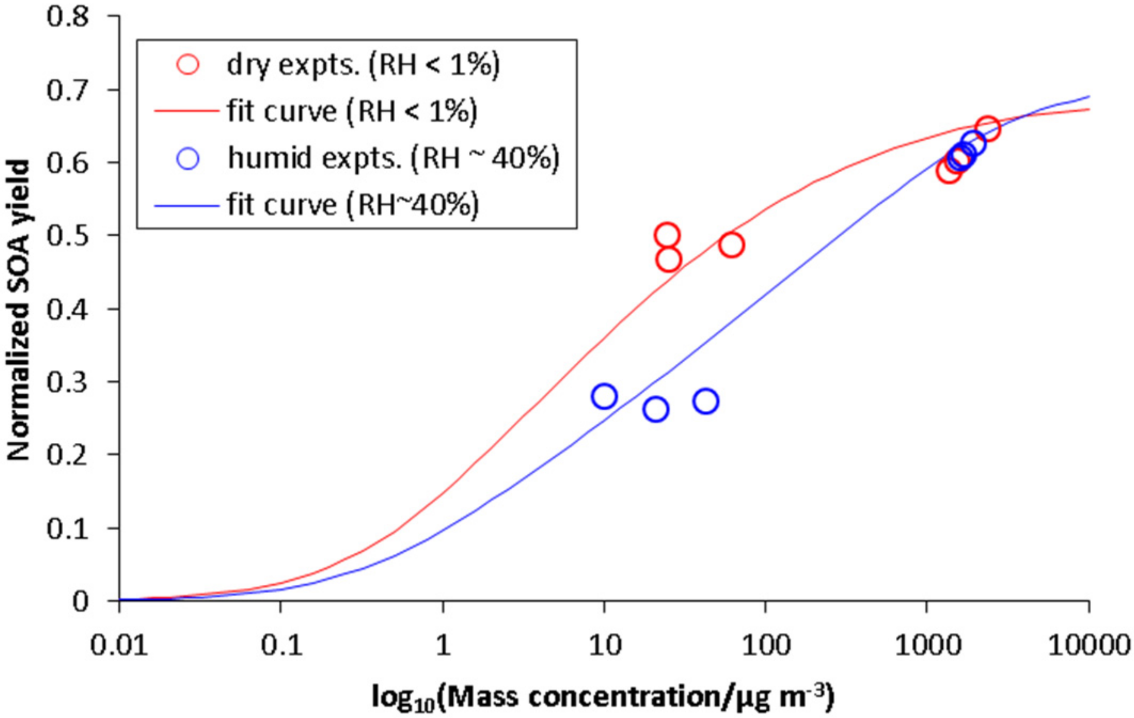

Figure S6: Normalized SOA yield measured as a function of mass concentration in dry (RH < 1%) and humid experiments (RH ~ 40%); the normalized SOA yields were corrected by accounting for particle wall loss in EDC. A partitioning theory function was used to fit experimental data (see text).

References

Sato, K., Jia, T., Tanabe, K., Morino, Y., Kajii, Y., and Imamura, T.: Terpenylic acid and nine-carbon multifunctional compounds formed during the aging of b-pinene ozonolysis secondary organic aerosol. Atmos. Environ., 130, 127-135, 2016.

Shiraiwa, M., Berkemeier, T., Schilling-Fahnestock, K. A., Seinfeld, J. H., and Pöschl, U.: Molecular corridors and kinetic regimes in the multiphase chemical evolution of secondary organic aerosol. Atmos. Chem. Phys., 14, 8323-8341, 2014.

Li, Y., Pöschl, U., and Shiraiwa, M.: Molecular corridors and parameterizations of volatility in the chemical evolution of organic aerosols. Atmos. Chem. Phys., 16, 3327-3344, 2016.